

# Effect of $H_3PO_4$ reactant and NaF additive on the crystallization and properties of brushite

C. Sekar<sup>1\*</sup>, K. Suguna<sup>2,3</sup>

<sup>1</sup>Department of Bioelectronics & Biosensors, Alagappa University, Karaikudi 630003, TN, India

<sup>2</sup>Department of Physics, Sri Sarada College for Women, Salem 636016, TN, India

<sup>3</sup>Department of Physics, Periyar University, Salem 636 011, TN, India

\*Corresponding author. Tel: (+91) 9442563637; E-mail: [sekar2025@gmail.com](mailto:sekar2025@gmail.com)

Received: 24 Jan 2011, Revised: 30 March 2011 and Accepted: 08 May 2011

## ABSTRACT

Calcium hydrogen phosphate dihydrate ( $CaHPO_4 \cdot 2H_2O$ , CHPD) or brushite crystal is a well known urinary substance found frequently in urinary stones. The CHPD crystals have been crystallized in sodium metasilicate gel (SMS) at room temperature under pH 6 in the presence of sodium fluoride. Here,  $H_3PO_4$  and  $CaCl_2$  were used as reactants which resulted in simultaneous crystallization of mostly dendritic brushite crystals and a small quantity of hydroxyapatite (HA). On the other hand, use of  $Na_2HPO_4$  and  $CaCl_2$  as reactants yielded large quantity of HA along with platelet brushite crystals. In both the cases, addition of sodium fluoride is found to inhibit the nucleation and subsequent growth of brushite crystals. The crystal morphology, structure and elemental composition of the grown crystals have been analyzed using SEM-EDX and powder XRD studies. Functional groups present in the grown crystals have been confirmed from the vibrational frequencies of the recorded FTIR spectrum. Copyright © 2011 VBRI press.

**Keywords:** Brushite; gel growth; sodium fluoride; X-ray diffraction; FTIR.



C. Sekar is currently Professor and Head, Department of Bioelectronics and Biosensors at Alagappa University, Karaikudi. He received his Ph.D. in Physics from Anna University, Chennai in the year 1997. His research interests include semiconductor nanostructures, carbon nanotubes, biomaterials and biosensors. He has published over 50 research papers in reputed international journals.

## Introduction

Biom mineralization phenomena are the root cause of several diseases in humans; the common examples are crystal-induced urinary calculus, calcified plaque in the arteries, gall bladder stone, etc [1, 2]. Renal stone or urinary calculi disease is an ancient and common affliction found in industrialized nations. This common disorder of renal stone formation affects up to 15% of the population over a life time, and without proper treatment and preventive measures, approximately 75% of these patients will have at least one recurrence. In urinary calculus several crystalline components such as calcium oxalate, calcium phosphate and ammonium magnesium phosphate hexahydrate are found. Hydroxyapatite [HA,  $Ca_5(PO_4)_3(OH)$ ], octacalcium phosphate [OCP,  $Ca_8H_2(PO_4)_6 \cdot 5H_2O$ ], monetite [DCPA,

$CaHPO_4$ ] and brushite [CHPD,  $CaHPO_4 \cdot 2H_2O$ ] are different crystalline phases of calcium phosphates present in various concentrations in urinary stones [3].

Among these, CHPD plays a significant role in the formation of metabolic and non-metabolic urinary calculi. The increasing incidence of these diseases in people of all ages affecting the considerable number of the total population is a major social and economic problem. Recent innovations in health care have included a number of less invasive technologies for treating the urinary stone diseases previously managed by surgery. Many chemicals are found to inhibit the growth of urinary stones as well as crystals.

Fluoride ion in drinking water is known for both beneficial and detrimental effects on health [4]. A higher concentration causes serious health hazards. The disease caused manifests itself in three forms, namely, dental, skeletal, and non-skeletal fluorosis. In India, almost 60–65 million people drink fluoride contaminated groundwater and the number affected by fluorosis is estimated at 2.5 to 3 million in many states [5]. Effect of fluorides (NaF) on the crystallization of brushite and HA has been investigated in detail [6, 7]. The authors have concluded that the addition of sodium fluoride inhibits the nucleation and subsequent growth of HA and brushite. The authors have used  $Na_2HPO_4$  and  $CaCl_2$  as reactants which yielded large quantity of HA along with a small number of brushite crystals.

In the present work, we have investigated the crystallization of CHPD under *in vitro* conditions by using  $H_3PO_4$  (instead of  $Na_2HPO_4$ ) as one of the reactants. Influence of sodium fluoride (NaF) as additive on the growth, structure and spectral properties have been investigated. This type of study is important as the crystallization process depends very much on the ingredients and growth environment.

## Experimental

Gel is the most preferred medium for the *in vitro* crystallization of biomolecules because of their viscous nature which provides simulation of biological fluids. The gel frame work, which is chemically inert, acts like a three dimensional matrix or a container in which the crystal nuclei are held and supplied with different nutrients for growth. This method is considered as a simplified model to study the crystallization of urinary calculi *in vitro* [8].

The crystallization apparatus employed was glass test tubes of 25 mm diameter and 150 mm length for single diffusion method. The chemicals used were AR grade NaF,  $CaCl_2$  and  $H_3PO_4$ . The SMS gel or water glass was prepared as per the literature [9]. One of the reactants ortho phosphoric acid (1M  $H_3PO_4$ ) was mixed with silica gel of density  $1.06\text{ gm/cm}^3$  so that the pH of the mixture could be set to 6. The mixture was transferred into test tubes. After the gel set, the supernatant solution of 1M calcium chloride was slowly added along the walls of the growth columns (test tubes) over the set gels and tightly closed to prevent evaporation. To study the effect of fluoride, NaF (0.1 – 0.4M) was added along with calcium chloride. The test tubes were kept undisturbed in the ambient atmosphere and growth was monitored regularly for about three weeks.

Growth features of CHPD crystals were studied using scanning electron microscopy (SEM) and the elemental analyses were done using the OXFORD INCA energy dispersive X-ray fluorescence spectrometer. The surface of the crystal was coated with a thin layer of gold to make the sample conducting. Powder X-ray diffraction pattern was recorded on Bruker advance diffractometer with  $Cu\ K\alpha_1$  radiation ( $1.5406\text{ \AA}$ ) within the  $2\theta$  range of 10 to  $70^\circ$ . FTIR spectra of the grown crystals were recorded using Perkin Elmer, Spectrum Rx1 detector and KBr beam splitter with KBr pellets. Thermal analysis of samples was performed using simultaneous TG instrument with thermal solution versions 1.2J controller software. Data analysis was carried out using TA Instrument Universal Analyzer version 2.3C software.

## Results and discussion

### Crystal growth

Brushite crystals have been grown by gel method with and without NaF addition. In both the cases,  $H_3PO_4$  was used as a reactant which resulted in the formation of brushite crystals as the main product. There has been a significant change in the growth pattern and crystal yield when compared to the similar crystals grown using  $Na_2HPO_4$  as the reactant. In pure system, a white precipitate was observed at the gel- solution interface within 12 minutes of

pouring the supernatant solution. White colored Liesegang rings have appeared just below the interface within 6 hours. The numbers of these rings increased with time and a total of 16 such rings with approximate thickness of about 0.5 mm were observed. However, at the same time, the first few Liesegang rings started dissolving and tiny spherulitic crystals have grown in its place. Needle shaped CHPD crystals have grown in between the Liesegang rings. These crystals were colorless and transparent in nature. Approximately 10 -15 needle shaped crystals were harvested after three weeks [Fig. 1a]. Contrary to this, use of  $Na_2HPO_4$  as reactant yielded transparent platelet shaped crystals [6].

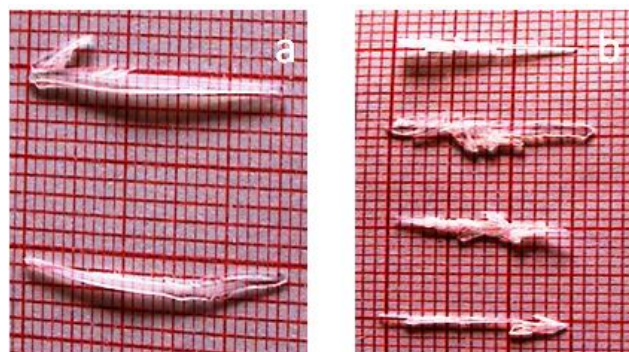


Fig. 1. As grown CHPD crystals (a) pure (b) 0.4M NaF added.

In case of fluoride added experiments, the thickness of the white precipitate and the number of Liesegang rings got decreased with the increase in sodium fluoride concentration. At lower concentration (0.1 M & 0.2 M) of NaF, the CHPD crystals started appearing within 2-3 days after pouring the supernatant solution which is similar to the pure system. Further increase in fluoride content (0.3 M & 0.4M) delayed the nucleation process and the tiny crystals started appearing only after 5 - 6 days. Accordingly, the crystal size and the number of crystals also decreased with increase in fluoride content [Fig. 1b]. Different additives are known to have different effects on the crystal growth; some additives or impurities can suppress growth; some may enhance growth [10]. Here the addition of NaF inhibits the crystal growth of CHPD and this may be due to blocking of active growth sites. This inhibitory nature was found to be independent on the chemical nature of the reactants.

### SEM-EDX studies

The scanning electron microscopic picture of a typical needle shaped CHPD crystal is shown in Fig. 2a. The crystal surface was found to be clean and free from any major crystal growth defects. The crystal habit and surface features of CHPD crystals grown with lower concentration of NaF additives (0.1M) resemble to that of pure system. Step-like growth pattern (Fig. 2b) has been observed in the crystals grown with higher concentration of fluorides (0.4M). This is possibly due to the incompleteness of crystal growth which can be attributed either to the non-availability of the solute particle at the growth interface during the growth or to the sudden termination of the growth. At higher concentrations, the excess fluoride ion may react with calcium resulting in the formation  $CaF_2$  [11]

which in turn leads to Ca deficiency in the supersaturated solution and hence the growth got interrupted.

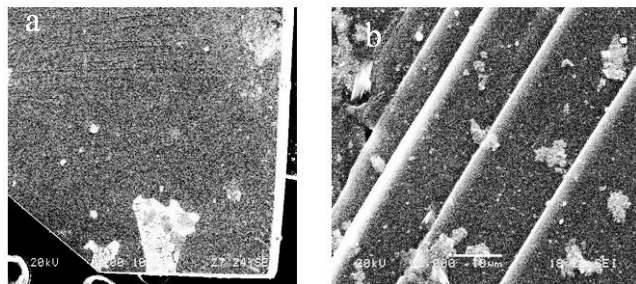


Fig. 2. SEM pictures of CHPD crystals (a) pure (b) 0.4M NaF added.

EDX measurements were made at different points on the crystal surface and the average atomic percentages of the individual elements are shown in **Table 1**. The result indicates that the crystal is composed of primarily calcium and phosphorous (**Fig. 3a&b**). The average calcium to phosphorus (Ca/P) ratio in the pure crystals is found to be 1.042, which is nearly equal to the expected value of 1.00 according to chemical formula. Similarly for crystals grown with 0.1 and 0.2M NaF, the Ca/P ratio was found to be nearly stoichiometric like that of pure crystal. However, the Ca/P ratio decreased with increase in NaF concentrations viz; 0.965 for 0.3M NaF and 0.909 for 0.4M [Table 1]. There is a significant increase in sodium and fluoride ion concentration with the increase in additive content. It should be noted that the Ca content in these crystals are less than the stoichiometric value. On the other hand, the Ca/P ratio of brushite crystals grown in presence of NaF by using  $\text{Na}_2\text{HPO}_4$  as reactant was reported to be nearly stoichiometric [6].

#### Powder XRD analyses

The powder X-ray diffraction pattern of white precipitate, spherulitic crystals and needle shaped crystals are shown in **Fig. 4**. The d values obtained from the reflections of white precipitate could be assigned to that of HA (JCPDS data 09-0432). The spherulitic crystals were found to be a mixture of monetite (JCPDS data 70-1425) and brushite. The XRD pattern of the needle shaped crystals agrees well with that of brushite (JCPDS data 72-0713).

Table 1. EDX analyses of pure and fluoride doped CHPD crystals

| Element     | Pure CHPD<br>(atm. %) | 0.3M NaF<br>(atm. %) | 0.4M NaF<br>(atm. %) |
|-------------|-----------------------|----------------------|----------------------|
| Ca          | 51.04                 | 44.01                | 37.23                |
| P           | 48.96                 | 45.62                | 40.96                |
| Na          | -                     | 1.96                 | 4.77                 |
| F           | -                     | 7.49                 | 15.89                |
| Si          | -                     | 0.92                 | 1.15                 |
| <b>Ca/P</b> | <b>1.042</b>          | <b>0.965</b>         | <b>0.909</b>         |

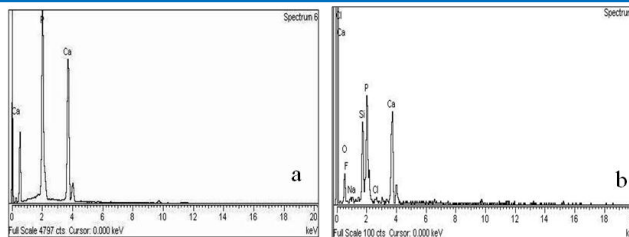


Fig. 3. EDX spectrum of CHPD crystals (a) pure (b) 0.4M NaF added.

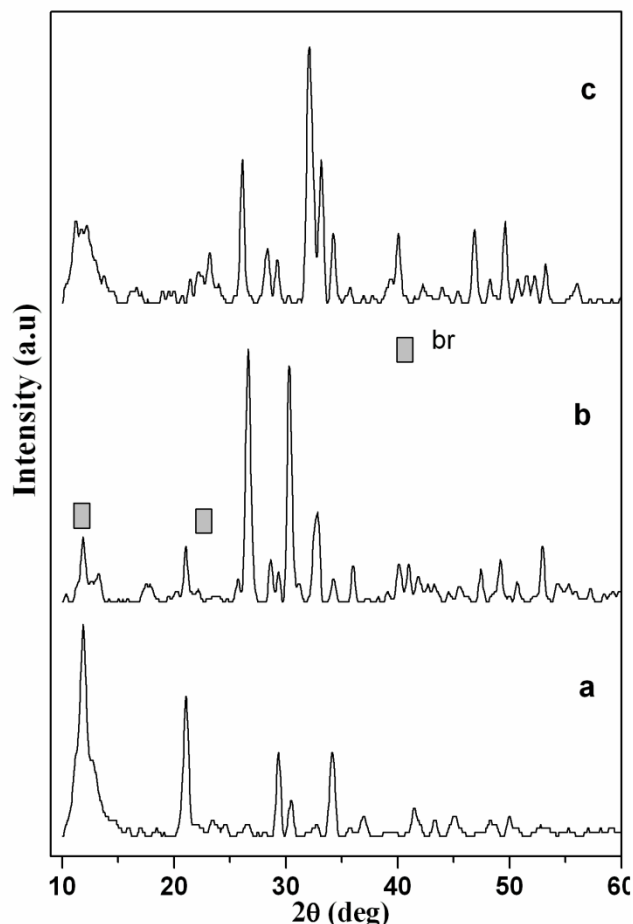
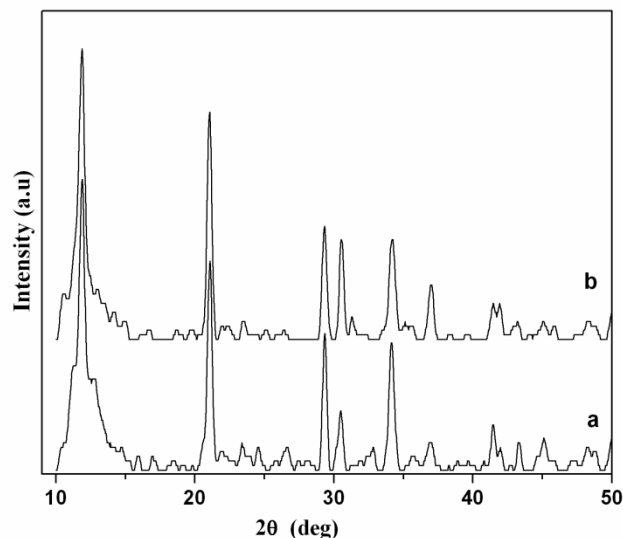


Fig. 4. Powder XRD patterns of (a) CHPD, (b) Monetite (c) HAP crystals grown without NaF addition.

The CHPD crystals are known to crystallize in the monoclinic system with space group  $Ia$  with the following lattice parameters,  $a = 5.812 \text{ \AA}$ ,  $b = 15.180 \text{ \AA}$ ,  $c = 6.239 \text{ \AA}$  and  $\beta = 116.25^\circ$  [12]. The powder XRD pattern of pure and fluoride doped CHPD crystals are shown in **Fig. 5**. All the observed peaks are in good agreement with the JCPDS (No. 72-0713) data. The lattice parameters were determined from the single-crystal X-ray diffraction data obtained with a four-circle Nonius CAD4 MACH3 diffractometer ( $\text{MoK}\alpha$ ,  $\lambda = 0.71073 \text{ \AA}$ ) [Table 2]. There has been a small shrinkage in volume which may be due to the loss of water and phosphate ions. Through the openings produced by the shrinkage the  $\text{F}^-$  ions may penetrate into the crystal [13].



**Fig. 5.** Powder XRD patterns of CHPD crystals (a) pure (b) 0.4M NaF added.

**Table 2.** Lattice parameters of pure and fluoride doped CHPD crystals

| Samples   | Lattice Parameters (Å) |          |          | Volume (Å <sup>3</sup> ) |
|-----------|------------------------|----------|----------|--------------------------|
|           | <i>a</i>               | <i>b</i> | <i>c</i> |                          |
| Pure      | 5.808                  | 15.176   | 6.236    | 492.5                    |
| 0.4 M NaF | 5.811                  | 15.170   | 6.230    | 491.5                    |

### FTIR studies

The recorded FTIR spectra for pure and fluoride doped CHPD crystal were depicted in **Fig. 6**. The observed wave numbers, relative intensities obtained from the recorded spectra and the assignments proposed for the crystals under investigation were found to be in good agreement with the reported literature [14, 15]. The detailed vibrational assignments were given in **Table 3**. The functional groups which play a prominent role in the observed IR spectra are discussed below. In the spectrum of pure sample, we can find two intense doublets: one with components at 3544 and 3489 cm<sup>-1</sup> and the other with components at 3284 and 3168 cm<sup>-1</sup>. In addition, a weak band around 2371 cm<sup>-1</sup> and a sharp strong band around 1652 cm<sup>-1</sup> has been observed. Presence of sharp band around 872 cm<sup>-1</sup> in all the IR spectra confirms the brushite mineral phase [14]. The sharp and strong band around 1652 cm<sup>-1</sup> is assigned to the bending of water molecules. Brushite is characterized by the splitting of phosphate bands in the region below 1600 cm<sup>-1</sup> with more doublets. At 989 cm<sup>-1</sup> a strong P–O stretching mode is observed. The two bands at 576 and 527 cm<sup>-1</sup> were assigned to P–O bending mode vibration. Appearance of minor peak around around 1215 cm<sup>-1</sup> is due to O–H bending of HPO<sub>4</sub> group. The band around 795 and 666 cm<sup>-1</sup> are due to librations of water molecules and are assigned to a rocking and wagging librational motion respectively.

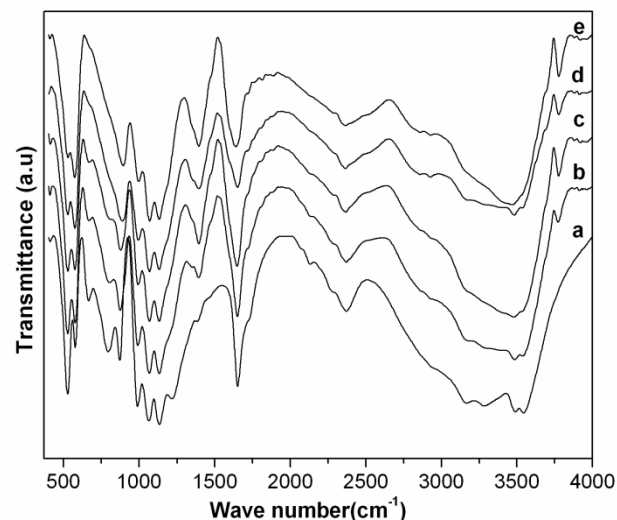


**Fig. 6** FTIR spectra of CHPD crystals (a) pure, and (b) 0.1M (c) 0.2M (d) 0.3M (e) 0.4M NaF added.

**Table 3.** Vibrational assignment of pure and fluoride added CHPD crystals.

| Pure CHPD | NaF Concentration |      |      |      | Vibrational assignments                                    |
|-----------|-------------------|------|------|------|--|
|           | 0.1M              | 0.2M | 0.3M | 0.4M |  |
| 3544      | -                 | -    | -    | -    | O–H Stretching (of water)                                  |
| 3489      | 3486              | 3480 | 3469 | 3483 | O–H Stretching (of water)                                  |
| 3284      | -                 | -    | -    | -    | O–H Stretching (of water)                                  |
| 3167      | -                 | -    | -    | -    | O–H Stretching (of water)                                  |
| 2371      | 2370              | 2367 | 2368 | 2366 | Combination  |
| 1652      | 1650              | 1647 | 1640 | 1653 | bending of water molecule                                  |
| -         | 1394              | 1395 | 1396 | 1397 | HPO <sub>4</sub> <sup>2-</sup> vibrations                  |
| 1217      | -                 | -    | -    | -    | Motion of hydroxyl group of HPO <sub>4</sub> <sup>2-</sup> |
| 1134      | 1133              | 1133 | 1132 | 1132 | P–O Stretching   |
| 1065      | 1067              | 1068 | 1069 | 1068 | P–O Stretching   |
| 989       | 991               | 994  | 997  | 995  | P–O Stretching   |
| 872       | 875               | 878  | 894  | 890  | P–O(H) Stretching  |
| 795       | 805               | -    | -    | -    | H <sub>2</sub> O Libration                                 |
| 666       | 669               | 669  | -    | -    | H <sub>2</sub> O Libration                                 |
| 577       | 576               | 575  | 574  | 575  | P–O Bending  |
| 527       | 527               | 527  | 529  | 527  | P–O Bending  |

The observed change over in the peak intensity of 3544 and 3489 cm<sup>-1</sup> for doped samples and the disappearance of doublet with components at 3284 and 3168 cm<sup>-1</sup> are attributed to the doping effect. The appearances of new peak around 3777 cm<sup>-1</sup> in all doped samples may be due to the presence of moisture in monetite and hydroxyapatite [16] as mixed phase. The peak around 1395 cm<sup>-1</sup> is attributed to the in plane bending of water molecule in the HPO<sub>4</sub><sup>2-</sup> ion. This peak becomes more prominent in the doped samples which again confirm the presence of other moist monetite in the fluoride grown samples. The peak at 1215cm<sup>-1</sup> in the case of pure CHPD crystal due to OH bending in the HPO<sub>4</sub> group has disappeared in all the doped cases. Intensity of the peak at 1652 cm<sup>-1</sup> decreases with the increasing concentration of the additive NaF. The peaks at 795 and 666 cm<sup>-1</sup> corresponding to (rocking and wagging) libration motion of water molecule disappeared completely in the doped samples. All these changes indicate the

significant influence of NaF on the growth and properties of calcium phosphate family crystals.

### Thermal analysis

Fig. 7 shows the TG-DSC curve of pure brushite recorded in the temperature range 30 -1000°C at the rate of 20°C/min in nitrogen atmosphere. In pure sample the weight loss occurs in two stages. The major weight loss of about 19% occurs between 141°C and 193°C which indicates the loss of water of hydration. Subsequently in the high temperature range of 193 - 468°C, two molecules of CaHPO<sub>4</sub> combine and result in the elimination of a water molecule leading to the formation of calcium pyrophosphate and nearly 74% of the sample is stable. The observed mass loss corresponds well with the DSC curve. The following chemical reactions are expected to occur during the dehydration and decomposition stages [17].

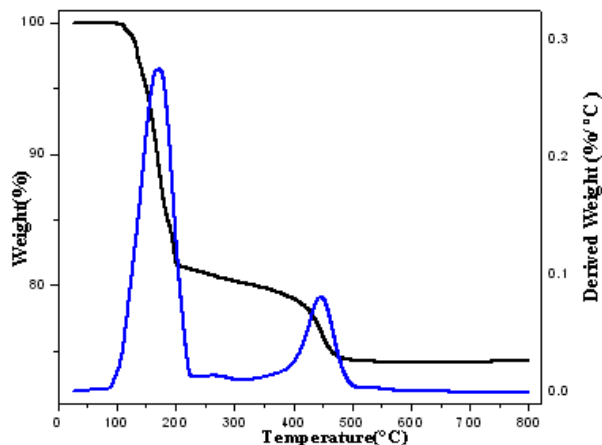
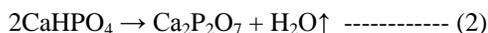


Fig. 7. TG-DSC curve of pure CHPD crystal.

There has been no significant change in the thermal behaviors for fluoride samples upto 0.3 M NaF. The brushite crystals grown with 0.4M NaF underwent a weight loss of about 18% between 120°C and 198°C. In the second stage nearly 5% weight loss occurred up to 468 °C and at the end 71% of the sample is stable. It can be noticed that the decomposition occurs at (120°C) a relatively lower temperature in the fluoride doped sample when compared to that of pure sample (141°C). Moreover, the total weight loss was higher in the doped sample. These results suggest that the thermal stability of brushite got reduced due to fluoride doping.

### Conclusion

Calcium hydrogen phosphate dihydrate crystals have been grown in SMS gel by using H<sub>3</sub>PO<sub>4</sub> and CaCl<sub>2</sub> as reactants. A small amount of HA and monetite have also got crystallized along with brushite. The presence of fluoride suppresses the nucleation and growth rate of CHPD

crystals. Powder XRD studies confirmed the phase formation and that there are no structural changes in the CHPD system due to doping. The EDX analyses showed that the calcium content decreases with the increase in NaF content in the growth environment. The Ca deficiency in brushite crystals have been attributed to the formation of CaF<sub>2</sub> in the fluorine rich environment. FTIR results confirmed that the fluoride is doped into CHPD and that the fluoride doping leads to the formation of moist monetite and hydroxyapatite as an admixture in the brushite crystal. TG-DSC analysis revealed that the fluoride doping decrease the thermal stability of brushite.

### Reference

- Robertson, W.G.; Peacock, M.; Hodgkinson, A. *J. Chron. Diseases*. **1979**, *32*, 469.  
DOI: [10.1016/0021-9681\(79\)90107-3](https://doi.org/10.1016/0021-9681(79)90107-3)
- Robertson, W.G.; Scurr, D.S.; Bridge, C.M. *J. Cryst. Growth*. **1981**, *53*, 182.  
DOI: [10.1016/0022-0248\(81\)90064-6](https://doi.org/10.1016/0022-0248(81)90064-6)
- Siva Kumar, G.R.; Girija, E.K.; Narayanakalkura, S.; Subramanian, C. *Cryst. Res. Technol.* **1998**, *33*, 197.  
DOI: [10.1002/\(SICI\)1521-4079\(1998\)33:2<197](https://doi.org/10.1002/(SICI)1521-4079(1998)33:2<197)
- Viswanathan, G.; Jaswanth, A.; Gopalakrishnan, S.; Siva ilango, S. *Science Total Environ.* **2009**, *407*, 1579.  
DOI: [10.1016/j.scitotenv.2008.10.020](https://doi.org/10.1016/j.scitotenv.2008.10.020)
- Subba Rao, N. *Environ. Monit. Assess.* **2009**, *152*, 47.  
DOI: [10.1007/s10661-008-0295-5](https://doi.org/10.1007/s10661-008-0295-5)
- Sekar, C.; Kanchana, P.; Nithyaselvi, R.; Girija, E. K. *Mater. Chem. Phys.* **2009**, *115*, 21.  
DOI: [10.1016/j.matchemphys.2008.11.020](https://doi.org/10.1016/j.matchemphys.2008.11.020)
- Kanchana, P.; Sekar, C. *J. Cryst. Growth*. **2010**, *312*, 808.  
DOI: [10.1016/j.jcrysgro.2009.12.032](https://doi.org/10.1016/j.jcrysgro.2009.12.032)
- Kalkura, S.N.; Vaidyan, V.K.; Kanakave, M.; Ramasamy, P. *J. Cyst. Growth*. **1993**, *132*, 617.  
DOI: [10.1016/0022-0248\(93\)90092-B](https://doi.org/10.1016/0022-0248(93)90092-B)
- Joshi, V.S.; Parekh, B.B.; Joshi, M.J. *J. Urol. Res.* **2005**, *33*, 80.  
DOI: [10.1007/s00240-004-0450-6](https://doi.org/10.1007/s00240-004-0450-6)
- Mullin, J.W. *Crystallization*; Third Edition, Butterworth-Heimann, London **1993**.
- Sarig, S.; Leshem, R.; Ben-Yosef, N. *Chem. Eng. Sci.* **1976**, *31*, 1061.  
DOI: [10.1016/0009-2509\(76\)87027-3](https://doi.org/10.1016/0009-2509(76)87027-3)
- Beevers, C.A. *Acta Crystallogr.* **1958**, *11*, 273.  
DOI: [10.1107/S0365110X58000670](https://doi.org/10.1107/S0365110X58000670)
- Chow, L.C; Brown, W.E. *J. Dental Research.* **1973**, *52*, 1220.  
DOI: [10.1177/00220345730520061001](https://doi.org/10.1177/00220345730520061001)
- Sauer, G.R.; Zunic, W.B. ; Durig, J.R. ; Wuthier, R.E. *Calcif Tissue Int.* **1994**, *54*, 414.
- Jingwei Xu.; Ian Butler, S.; Denis Gilson, F. R. *Spectrochim. Acta Part A.* **1999**, *55*, 2801.  
DOI: [10.1016/S1386-1425\(99\)00090-6](https://doi.org/10.1016/S1386-1425(99)00090-6)
- Tao, Y.; Dong, W.; Xianpeng, Z.; Xiaodong, X.; Nuo, Z.; Dan, W.; Lianguo, Y.; He, L.; Bin, D.; Wei, Q. *Adv. Mat. Lett.* **2010**, *1(2)*, 106.  
DOI: [10.5185/amlett.2010.4111](https://doi.org/10.5185/amlett.2010.4111)
- Joshi, V.S.; Joshi, M. *J. Cryst. Res. Technol.* **2003**, *38*, 817. ,  
DOI: [10.1002/crat.200310100](https://doi.org/10.1002/crat.200310100)

## **ADVANCED *MATERIALS Letters***

### **Publish your article in this journal**

[ADVANCED MATERIALS Letters](#) is an international journal published quarterly. The journal is intended to provide top-quality peer-reviewed research papers in the fascinating field of materials science particularly in the area of structure, synthesis and processing, characterization, advanced-state properties, and applications of materials. All articles are indexed on various databases including [DOAJ](#) and are available for download for free. The manuscript management system is completely electronic and has fast and fair peer-review process. The journal includes review articles, research articles, notes, letter to editor and short communications.

